Spreading dynamics of polymer microdroplets: A molecular-dynamics study

J. A. Nieminen[1] and T. Ala-Nissila[1,2]
[1]*Department of Physics, Tampere University of Technology, P.O. Box 692, FIN-33101 Tampere, Finland*
[2]*Research Institute for Theoretical Physics, University of Helsinki, P.O. Box 9 (Siltavuorenpenger 20 C), FIN-00014 University of Helsinki, Finland*
(Received 7 December 1993)

The dynamics of spreading of microscopic nonvolatile polymer droplets on surfaces has been studied by the molecular-dynamics method. Simulations have been performed for mixtures of solvent and dimer, solvent and tetramer, and solvent and octamer droplets. For solvent particles and dimers, the dynamical layering is characteristic with stepped droplet shapes. However, for tetramers and octamers a tendency for layering is evident for relatively deep and strong surface potentials only, with one layer developing. For wider and more shallow potentials more rapid spreading and rounded droplet shapes occur, due to mixing of the layers. These results suggest that the molecular structure of the liquid may play a role in determining different experimentally seen density profiles of nonvolatile droplets.

PACS number(s): 68.10.Gw, 05.70.Ln, 61.20.Ja, 68.45.Gd

I. INTRODUCTION

Spreading of a liquid droplet on a solid surface is a more complex phenomenon than was originally believed. First, descriptions of wetting of a surface by liquid [1] assumed a spherical cap shape for the droplet. A step further was the discovery by Hardy [1] of a thin molecular film (precursor) preceding the macroscopic cap. Most recent experiments on the dynamics of spreading of tiny nonvolatile droplets have revealed even more complex and fascinating phenomena, including a variety of droplet shapes on molecular scales [2–8].

In the experiments, several different types of polymer liquids and surfaces have been used. The results show clearly that different liquids may spread in different ways on the same substrate as seen in Fig. 1 [2]. A droplet of polydimethylsiloxane (PDMS) [Fig. 1(a)] develops a monolayer thick precursor layer, while tetrakis (2-ethylhexoxy)-silane [Fig. 1(b)] develops a more complicated profile with multiple (up to four) precursor layers, and a tiny cap in the center of the droplet. Comparisons between flatter PDMS and squalane droplets reveal a "Mexican hat" shape for the former (i.e., a single layer with a central cap), and a more rounded shape for the latter, approaching Gaussian at late times [3]. In addition, more systematic studies of a variety of PDMS liquids yield "stepped pyramid" (layered) profiles on grafted silicon surfaces [7].

On the other hand, there are differences even for the same liquid on different substrates. In Ref. [4], PDMS develops dynamical layering on a "high energy" surface, while only one precursor layer is observed on a "low energy" surface. In another experiment with chemically modified PDMS droplets [6], steps are observed on two different silicon wafers. Furthermore, in a recent measurement of PDMS on a silver substrate [Fig. 1(c)] the droplet develops a spherical cap shape with Gaussian tails at late times [5]. Even more complicated shapes are possible [6–8].

From the experiments, a natural question then arises regarding reasons behind the different morphologies. One of the key issues is the occurence of dynamical layering on the scale of molecular layers. This cannot be explained by the usual continuum theories of spreading [1,9–11], but there is a need for more microscopic models. Dynamical layering can be obtained from the layered flow model of de Gennes and Cazabat [12] which assumes velocity differences and friction between layers, and interlayer permeation flow near droplet edges. Parameters associated with the model have recently been extracted [7] from stepped profiles of spreading droplets. The horizontal solid-on-solid (SOS) model [13,14] also yields dynamical layering, with the layer thickness determined by the range and the strength of the surface potential in the complete wetting regime. Another modified SOS model [15] manages to yield droplet profiles from rounded to layered shapes by varying a parameter, which controls interparticle and surface interactions, and interlayer flow. Rounded shapes occur for weaker interactions and larger interlayer flows, while increased attractive interactions enhance layering.

A more microscopic picture is given by molecular-dynamics simulations, which have been performed on simple models [16–18]. In particular, Nieminen *et al.* [18] simulated Lennard-Jones particles and were able to observe the appearance of a precursor film, dynamical layering, and a crossover from "almost linear" ($\sim t^{0.9}$) to "diffusive" ($\sim t^{0.5}$) behavior for the width of the precursor film [9,11]. None of the simulations up to date, however, take into account effects arising from the internal degrees of freedom of the molecules. Namely, in the experiments polymer fluids with different molecular structures are often used. It is well known, that for longer polymer chains the *excluded volume interaction* and *entanglement of chains* are important for a correct dynamical description [19]. In most cases, the fluids used

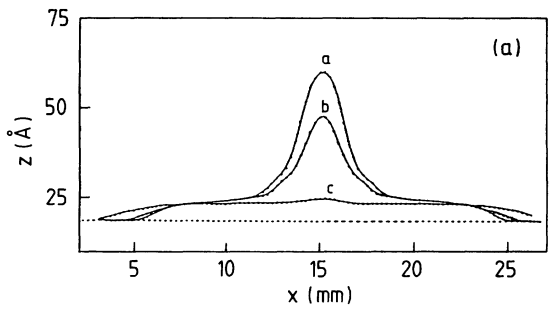

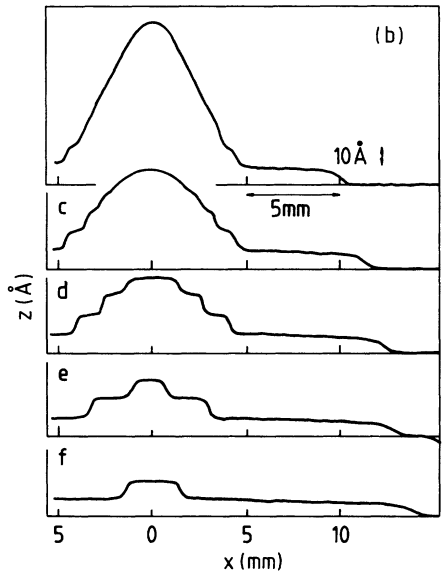

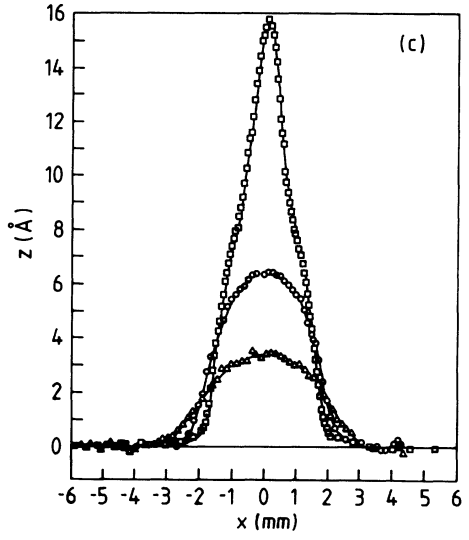

FIG. 1. Experimental density profiles for (a) a tiny PDMS droplet and (b) a tetrakis droplet on silicon (Ref. [2]). Dynamical layering for tetrakis is evident. (c) Density profiles for a PDMS droplet on silver surface (Ref. [5]). The late time profiles can be fitted with a spherical cap, with Gaussian convolution at the edges.

in the experiments show no particular polymeric effects in bulk equilibrium. Thus, actual entanglement should not play any role. However, it has recently been demonstrated that rounded (non-Gaussian) droplet shapes for late submonolayer stages of spreading can occur because of strongly blocked diffusion of short, unentangled polymer chains on surfaces [5,20]. This suggests that even for relatively short chains, spreading dynamics may become nontrivial in the sense that the internal degrees on freedom of the molecules can influence droplet profiles. In addition, there exists no systematic study on the influence of the strength of the surface potential on spreading dynamics in the complete wetting regime.

In this work our aim is to study these two questions, namely, the effect of the actual chain structure of the molecules, and the strength of the substrate potential on spreading dynamics of tiny liquid droplets. We will explicitly demonstrate that droplets of *solvent particles* (single atoms) and *flexible chains* can lead to rather different morphologies in microdroplets, even for relatively short chains. Namely, for solvent particles and rigid dimers, stepped shapes of the density profiles tend to occur, which is an indication of dynamical layering. For longer molecules of four (tetramers) or eight connected atoms (octamers), the internal degrees of freedom of the chains are shown to influence spreading dynamics and microdroplet morphologies. Our results show that even for these relatively short chains, *dynamical mixing* of the molecular layers may occur, leading to more rounded droplet shapes. This is favorable for relatively weak surface potentials and stiff chains, and it tends to preempt dynamical layering since different layers get mixed. On the other hand, if the attraction of the surface becomes strong enough to force the chains to lie parallel to it, indications of layering occur. We also demonstrate that if solvent particles are present in large concentrations, tendency towards dynamical layering is restored. Finally, we also discuss the effects of systematically varying the flexibility of the chains, and the temperature. A preliminary account of these results is given in Ref. [21].

II. THE MODEL

To study the most general case we consider a mixture of N_s "solvent" particles (single atoms), and N_p "polymers" (n-mers) which interact with each other via a Lennard-Jones (LJ) potential:

$$V_f = \epsilon_f \left[\left(\frac{\sigma_f}{r} \right)^6 - \left(\frac{\sigma_f}{r} \right)^{12} \right], \tag{1}$$

with potential parameters σ_f and ϵ_f for the width and the depth of the potential, respectively. The n-mers consist of n LJ particles, which are interconnected by a very rigid but orientationally isotropic harmonic oscillator pair potential $V_c = \frac{1}{2}k(r-r_0)^2$, where $r_0 = 2^{\frac{1}{6}}\sigma$ and $k = 100\epsilon_f/\sigma_f^2$ or $10000\epsilon_f/\sigma_f^2$ so that the chains do not easily stretch. There is also an angle dependent potential $V_\theta = \epsilon_\theta(\cos\theta + 1)$, for $n > 2$, where $\cos\theta = \hat{r}_{ij} \cdot \hat{r}_{ik}$, and

$\hat{r}_{ij}$ is the unit vector from atom i to its nearest neighbor j. For our studies we examine three cases, namely, $\epsilon_\theta = 10\epsilon_f$ (rather stiff chains), $\epsilon_\theta = 0.14\epsilon_f$ (rather flexible chains), and $\epsilon_\theta = 0$ (freely bending chains). For the purposes of the present work, an essential feature in this simplified polymer model is that due to the strong repulsive core between atoms comprising an n-mer, strong repulsion is created if the chains try to spatially overlap. Our model should also correctly incorporate effects arising from the excluded volume interaction in real polymer chains [5,19,20].

The substrate is modeled by a flat continuum LJ material, since a moderate corrugation does not essentially change the spreading pattern for solvent droplets [18]. The substrate is thought to be homogenous and its unit volume $\Omega = 1$. The total substrate interaction is obtained by integrating the LJ potential over the half space $z < 0$:

$$V(z) = -\frac{\mathcal{A}}{z^3} + \frac{\mathcal{B}}{z^9}. \tag{2}$$

Interaction parameters $\mathcal{A}$ and $\mathcal{B}$ are now functions of the LJ parameters: $\mathcal{A} = (2\pi/3)\epsilon_s\sigma_s^6$ and $\mathcal{B} = (4\pi/45)\epsilon_s\sigma_s^{12}$. It can be shown that for the substrate-fluid interaction, the depth of the potential is comparable to $\epsilon_s\sigma_s^3$ and the width to σ_s (see Ref. [18]).

The dynamics of the system is described by the usual equations of motion [18,22]:

$$\frac{dr_i}{dt} = \frac{p_i}{m_i}, \tag{3}$$

$$\frac{dp_i}{dt} = \nabla_i V - \eta p_i, \tag{4}$$

and

$$\frac{d\eta}{dt} = \left[\sum \frac{p_i^2}{m_i} - NkT\right] \Big/ NkT\tau^2, \tag{5}$$

where N is the number of degrees of freedom, T the temperature for the thermostat, and τ is a relaxation time. The time scales here have been chosen in the same way as in Ref. [18]. Initially a ridge-shaped droplet is constructed with periodic boundary conditions along the direction of the ridge. The spreading takes place in the direction perpendicular to the ridge. The equations of motion are solved using modified velocity Verlet algorithm (see, e.g., Refs. [23] and [24]). In simulations reduced time units (r.u.) are used, which in this work are defined as $t(\text{r.u.}) = 2 \times (1\ \text{Å})\ \sqrt{(1\ \text{amu})/(1\ \text{eV})} \approx 0.066$ ps.

Due to the complex topology of the n-mer droplets, constructing the initial configuration of the droplet is not straightforward. An optimal packing of the molecules must be found before the droplet is allowed to spread. In the beginning the n-mers are arranged to a form of a spherical droplet, and they are bent 90° at each joint, while their directions are random. The initially rather sparse system is then compressed to find the minimum of the internal energy. Finally, the droplet is allowed to thermalize, for a time comparable to the spreading simulation. Then the substrate potential is "switched on" and the spreading can take place.

In practice, this procedure does not lead to the globally optimal packing, since rearrangement of chains may require a very long relaxation time. For longer chains, the initial configurations contain many locally optimal domains, with small voids between them. They may cause fluctuations in the data, especially for octamers. Our test runs show that sparser droplets spread slightly slower than dense ones. This is taken into account in the analysis when necessary. We note that all our presented data displays universal crossover scaling (cf. Sec. III C), which is an indication that packing effects are relatively unimportant.

III. RESULTS

In the previous study of Nieminen *et al.* [18] the temperature was $kT_s = 0.8\epsilon_f$, which is well above the triple point of an LJ material [25]. In the present case the larger mass and binding energy of the n-mers allows us to systematically vary *both* the surface potential *and* the temperature, and thus, e.g., study the effects of changing the viscosity of the "polymer" liquid. In all cases here, the fluid remains nonvolatile. In the present work, we employ four sets of substrate interaction parameters: $\epsilon_s = 5\epsilon_f$ and $\sigma_s = \sigma_f$ (used in Ref. [18]), denoted as S_{I}; $\epsilon_s = \epsilon_f$ and $\sigma_s = 5.0\sigma_f$ (S_{II}); $\epsilon_s = 0.02\epsilon_f$ and $\sigma_s = 7.3\sigma_f$ (S_{III}); and $\epsilon_s = 0.002\epsilon_f$ and $\sigma_s = 7.3\sigma_f$ (S_{IV}). The differences between these potentials can be characterized by their steepness (gradient) ($\sim \epsilon_s{\sigma_s}^2$), depth, and width. All four potentials are depicted in Fig. 2. S_{I} is rather narrow, while S_{II} is much deeper than the other potentials. S_{III} and S_{IV} are both relatively shallow and wide, the latter being particularly flat. In addition, we also vary the relative concentrations of solvent particles and n-mers. The total number of particles $N = N_s + nN_p$, and the concentration of chains is denoted below by $c = nN_p/N$. Typically, N is of the order of 10^3.

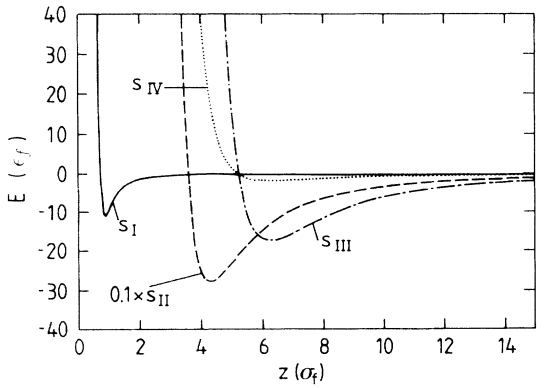

FIG. 2. The four distinct surface potentials used in the present work. For clarity of presentation, S_{II} has been multiplied by 0.1. See text for details of the LJ parameters.

A. Qualitative features of spreading

1. *Mixtures of dimer and solvent droplets*

First, we discuss the spreading dynamics of solvent and dimer droplets, whose behavior turns out to be rather similar. To compare with, simulations for pure solvent droplets (LJ particles) were done in Ref. [18] for $S_{\rm I}$. It was observed there that the width of the precursor film $w(t)$ started "adiabatically," i.e., following t^x, where $x \approx 0.9 - 1.0$ [11]. Crossover from adiabatic to "diffusive" $x \approx 0.5$ spreading was observed after some time. Evidence for dynamical layering was also seen by examining snapshots of atomic configurations. However, no quantitative analysis was performed.

Qualitatively, our present results show that a dimer concentration of 50% or 100% does not alter the essential features of spreading as compared to a pure solvent droplet (see Fig. 3). Most importantly, dimer droplets and their mixtures exhibit rather well separated layers for $S_{\rm I}$, $S_{\rm II}$, and $S_{\rm III}$. In order to observe clear separation of molecular layers for pure dimer droplets the deeper substrate potential $S_{\rm II}$ must be used (for $S_{\rm I}$ only a single precursor layer forms). An interesting feature of the spreading dynamics is the orientation of the dimer molecules along the flow perpendicular to the surface. For the case of $S_{\rm II}$, where layer separation is most clearly seen, attraction at the surface level is strong enough to orient the dimers parallel to the surface plane. For this case, the larger spring constant has been used to avoid collapse of chains. For the shallower and wider potential $S_{\rm III}$, the dimers remain perpendicular to the surface for long times, which tends to mix the layers somewhat. However, this does not affect layer separation very much as seen in Fig. 3. Despite the slight differences, all the dimer droplets show a crossover less distinct but similar to that observed for solvent particles for $w(t)$. The presence of dimers, however, makes the spreading dynamics slightly slower.

2. *Mixtures of tetramer and solvent droplets*

In the case of tetramers, we have mostly studied the cases of rather stiff and rather flexible polymers. Effects arising from the chain structure of the liquid become more apparent. The dynamical orientation of the chains along the "flow" of the spreading droplet is now very clear, in particular for the stiffer chains of Fig. 4, and stronger attraction of $S_{\rm II}$ [Figs. 4(a) and 4(b)]. This in part leads to dramatic changes in the structure of the layers. Namely, only for the very strong surface potential $S_{\rm II}$ does a clear precursor layer with a thickness of about one monolayer form. For this case also, the larger spring constant was used. When the surface potential becomes more shallow, a change in the droplet shapes occur. For $S_{\rm III}$ a vertically continuous precursor layer whose effective thickness is about two layers is seen. When the substrate potential is further weakened to $S_{\rm IV}$, the two layers tend to merge together. This leads to a noticeably more rounded droplet configurations than for dimers, as seen in Figs. 4(c) and 4(d). The rate of spreading of the droplet also becomes faster from $S_{\rm II}$ to $S_{\rm III}$, while no further increase in the rate is observed for $S_{\rm IV}$.

These results are consistent with the observation that for a strongly attractive, narrow surface potential the tetramers become packed *parallel* to the surface, which slows down their migration. This also promotes layer separation, but may eventually lead to spherical droplet shapes when the spreading becomes purely diffusive un-

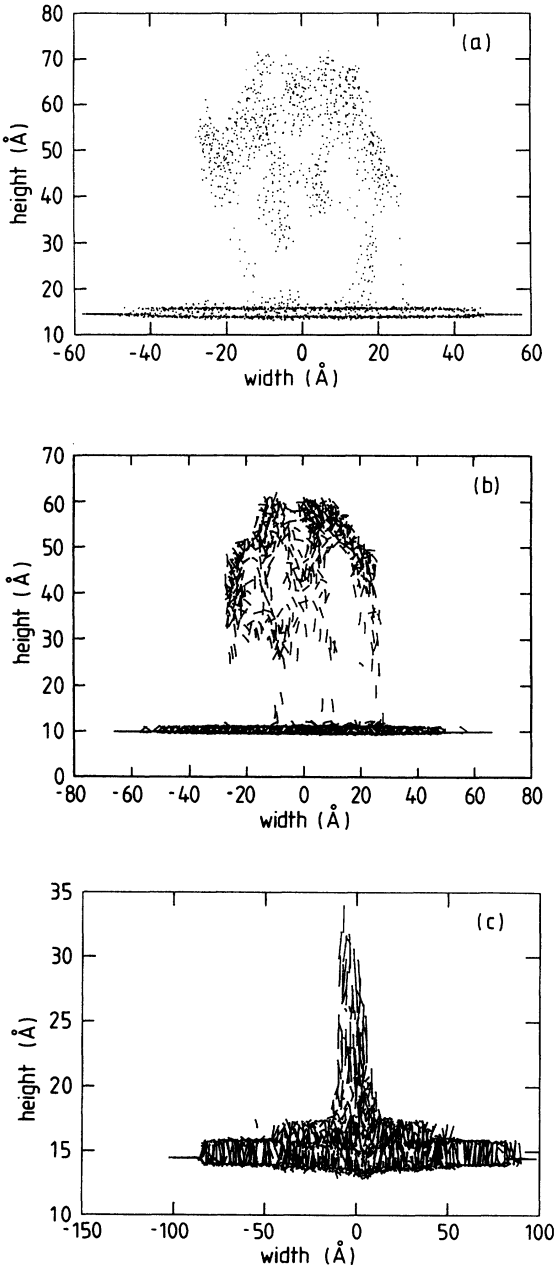

FIG. 3. Snapshots of spreading of monomer droplets for potential (a) $S_{\rm II}$ and pure dimer droplets for potentials (b) $S_{\rm II}$ (with larger k), and (c) $S_{\rm III}$. Separation of layers is apparent in both cases. The snapshots are taken at times 25, 25, and 50, respectively, in reduced units (r.u.). See text for details.

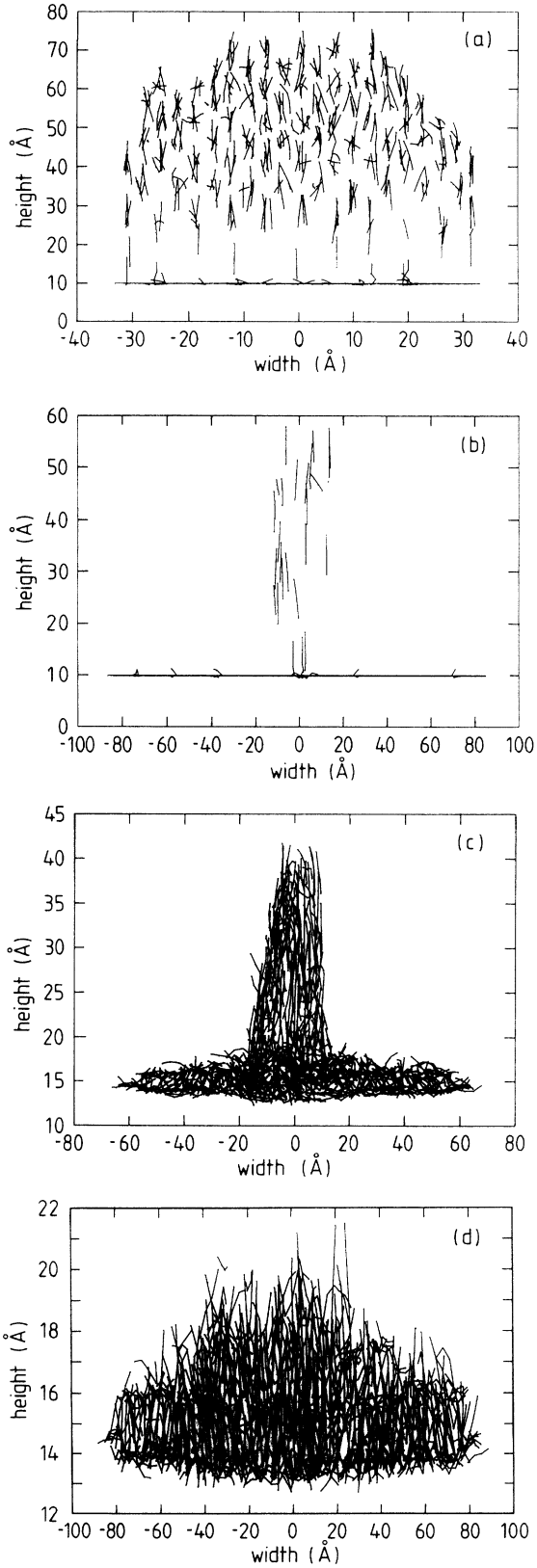

FIG. 4. Snapshots of spreading of pure tetramer droplets for potentials (a) and (b) S_{II} (larger k), and (c) and (d) S_{IV}, with rather stiff chains. The mixing of layers is evident in the latter case, which leads to a complex structure within the precursor layer. The times for snaphots are 25, 62.5, 50, and 75 r.u., respectively.

der submonolayer conditions [5,20]. On the other hand, a weaker surface potential does not force the tetramers in layers, thus allowing faster dynamics and formation of a more rounded droplet configuration at intermediate times. Mixing of the chains in the two layers is seen, which leads to the complex structure evident in Fig. 4(d).

When the concentration of solvent particles is increased, tendency towards layer separation is restored, and the spreading dynamics becomes faster. In Fig. 5 we show a comparison of the width of the precursor $w(t)$ for three different tetramer concentrations: $c = 0.0$, 0.5, and 1.0, where c denotes the fraction of LJ particles in the chains. These curves are qualitatively similar to the dimer cases, where crossover behavior occurs (cf. Sec. III C).

3. Mixtures of octamer and solvent droplets

In the case of octamers (see Fig. 6), problems with initial packing and smaller number of chains make a detailed analysis difficult. Nevertheless, the features of spreading dynamics are very similar to tetramers. High concentrations of rather stiff chains and weaker surface potentials favor interlayer mixing, which promotes more rounded droplet shapes. For $c = 0.5$, on the other hand, slight traces of layer separation can be seen. The spreading dynamics becomes faster, too, but only slightly. This seems to be due to a stronger mixing of the longer chains.

The effect of chain flexibility was examined for $c = 1$ and $1/2$ for the cases of rather stiff and completely flexible chains. For pure octamer droplets ($c = 1$) there is a transient time where a droplet with rather stiff chains spreads about twice as fast as a droplet with completely flexible chains. After this transient both droplets seem to reach roughly the same spreading rates.

B. Analysis of density profiles

Next, we analyze density profiles of the droplets in order to make comparison with experiments [2–7]. The

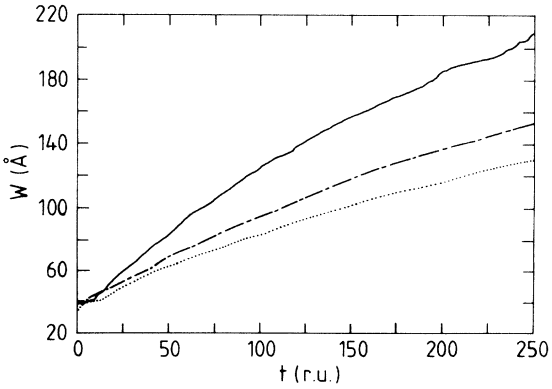

FIG. 5. Width of the precursor layer $w(t)$ vs time for tetramer droplets, with concentrations $c = 0$ (solid line; a pure solvent droplet), $c = 0.5$ (dash-dotted line), and $c = 1.0$ (dotted line). Despite the slowing down of the spreading rate, each case shows similar crossover behavior (cf. Fig. 9). The reduced time units (r.u.) are defined in the text.

density is defined as the number of particles per unit area on the surface. As seen in Fig. 7(a), the density profile for a typical solvent droplet shows a stepped precursor layer for S_{II}, indicating separation of layers. Results for dimers are analogous, with some rounding off at the step edges for S_{III} [Fig. 7(c)], as compared to S_{II} [Fig. 7(b)]. The layers nevertheless remain rather well separated.

For tetramers in the case of S_{II}, the density profiles of the rather stiff chains are shown in Fig. 8(a). An indication towards a stepped "pyramid" structure of the intermediate time profiles is seen. The same applies to rather flexible chains, too, although the shoulders in the profiles are less distinct. For weaker potentials, however, the mixing of the layers seen in the configuration snapshots becomes manifest. For potentials S_{III} and S_{IV} the precursor film on the whole is fairly thick and the density increases rather continuosly towards the center, forming a rather smooth cap at late stages. Only a single shoulder is visible in Fig. 8(b). For the rather flexible chains of Fig. 8(c) the profiles are even smoother. At the latest times studied (not shown in Fig. 8), a slight density gap in the middle of the droplet is formed for the weaker potentials. This is probably a finite size effect.

Density profiles for octamers are very similar to tetramers, except that stronger finite size and packing effects make the analysis more difficult. In particular, even for the rather stiff chains, at late times there is a region of lower density in the middle of the droplet. For completely flexible chains in the weaker potentials, chains in the middle are pushed aside and the density peaks at the edges of the droplet.

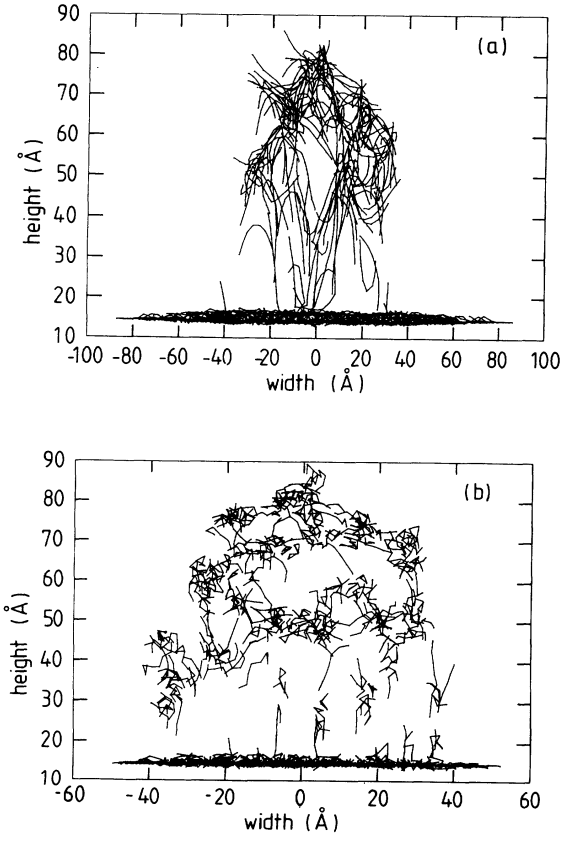

FIG. 6. Snapshots of spreading of pure octamer droplets for (a) rather stiff and (b) completely flexible chains, in the case of S_{III}. In both cases, mixing of layers is visible, similar to the case of tetramers. Times are 25 r.u. in both cases.

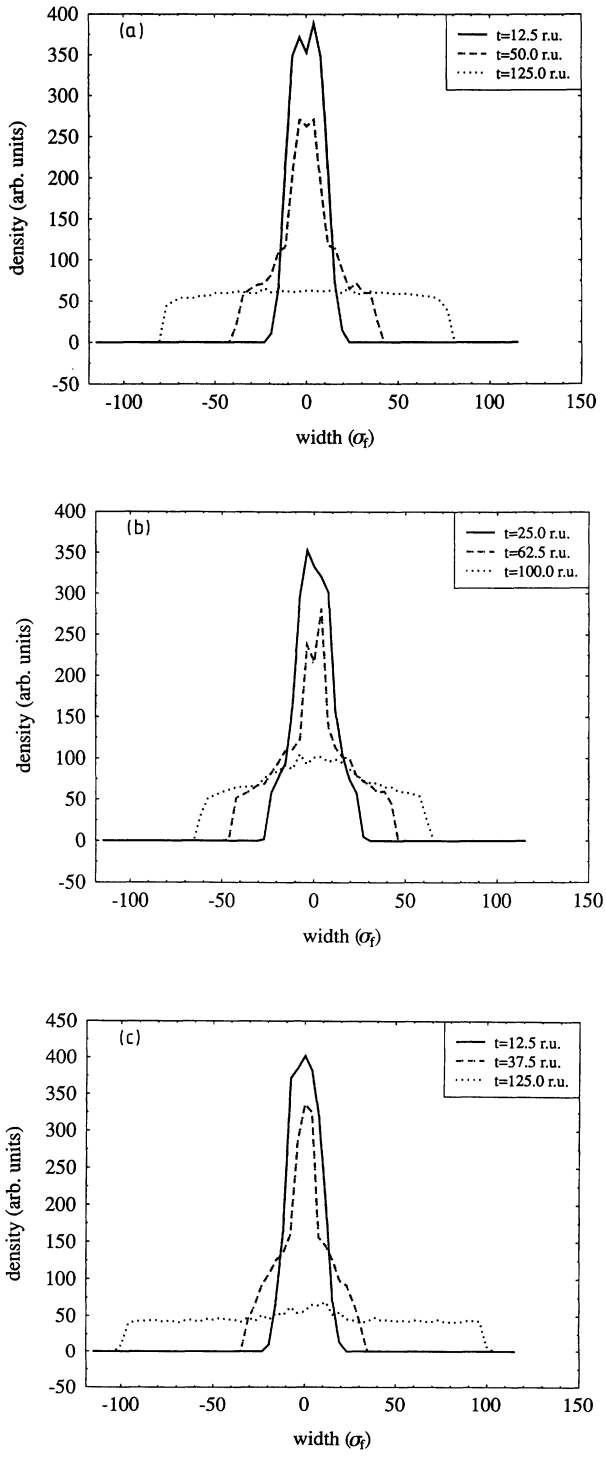

FIG. 7. Density profiles for (a) a solvent droplet with S_{II}, (b) a pure dimer droplet with S_{II}, and (c) a pure dimer droplet with S_{III}. In each case, dynamical layering occurs.

The profiles of Figs. 7 and 8 bear a remarkable qualitative resemblence to some of the experimentally measured ones. The stepped profile of Fig. 7(a), for example, is qualitatively very similar to that of a tetrakis droplet consisting of star-shaped molecules [2]. This is in complete accordance with the observation that in our microdroplets, for spherical or rigid molecules (dimers) separation of layers and dynamical layering tend to occur. On the other hand, the stepped profile of Fig. 8(a) is similar to PDMS droplets of grafted silicon surfaces [7,8]. The thickness of the individual layers in the experiments indicates that the PDMS molecules are lying flat on the surface. This is in agreement with what happens with our strongly attracting potential S_{II}.

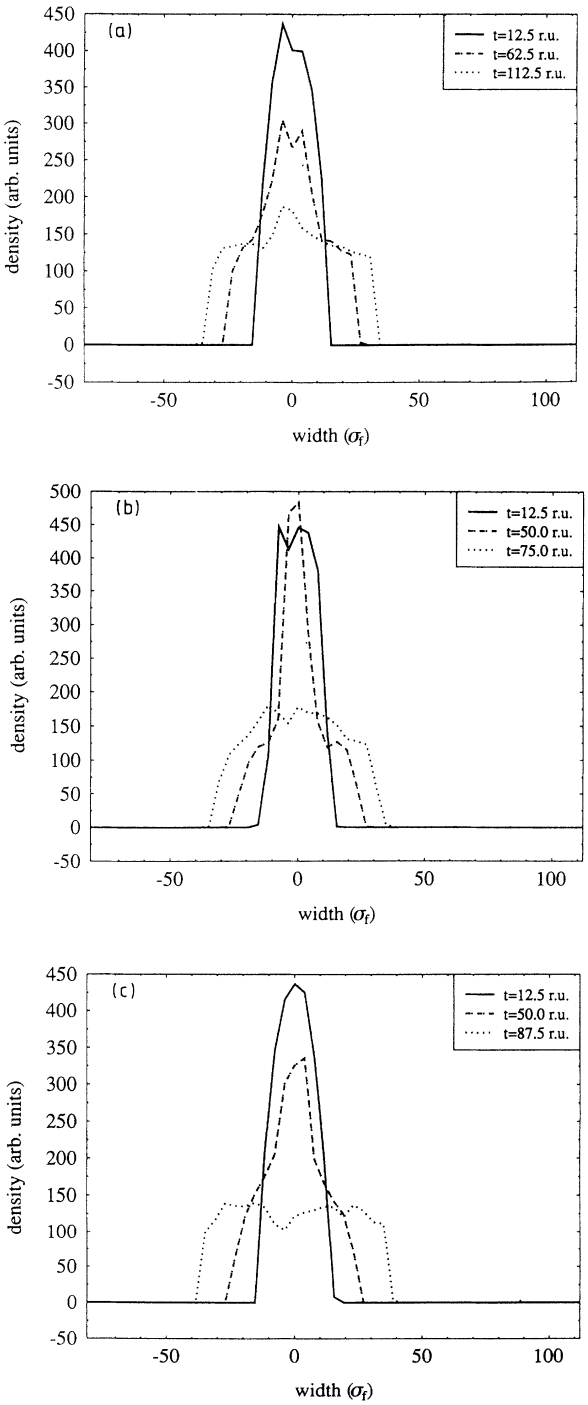

FIG. 8. Density profiles for pure tetramer droplets in potentials (a) S_{II} (rather stiff chains); (b) S_{IV} (rather stiff chains), and (c) S_{III} (rather flexible chains). Rounded droplet shapes for the weaker potentials are evident; see text for details.

The other profiles of the tetramer droplets [Fig. 8(c), in particular] resemble the rounded shapes of PDMS on silver [5] and on silicon surfaces [3]. Our results suggest that these profiles are more characteristic for chain-like flexible molecules, when the surface attraction is not too strong. However, spherical shapes can also occur for chains lying flat on the surface at late submonolayer stages of spreading, as demonstrated in Refs. [5] and [20]. Furthermore, on silicon a change of a PDMS droplet from a rounded towards a stepped shape was observed on a "high-energy" surface [4]. Our results suggest that this indicates increased substrate attraction, which tends to separate the layers. This is in accord with conclusions drawn from diffusion measurements of the same experiment [4].

It should be kept in mind, however, that quantitative comparisons of our results with the experiments are difficult, since experimental droplets are microscopic in the vertical direction *only*. Also, microscopic details of the surfaces and polymer liquids have not been reported in many cases, which makes it difficult to estimate the influence of various possible factors. The experimental situation remains complicated and should not be oversimplified. Nevertheless, our results indicate that the profile shapes are influenced not only by the surface attraction, but also the molecular structure of the fluid. They also support the conclusion that *weakening* the surface potential causes faster spreading rates [13] and more rounded droplet shapes for polymeric liquids.

Finally, we have also studied the effect of temperature. As expected, increasing the temperature reduces the effective viscosity and thus increases the spreading rates. For solvent and dimer droplets (S_{II}) changing the temperature from $T = T_S$ to $T = 1.5T_S$ simply makes the steps more rounded. For tetramer droplets the effects are relatively small. The high temperature mainly causes a more visible depression at the center of the droplet profiles at the late stages of spreading also for the rather stiff chains.

C. Finite size scaling of the precursor width

An interesting question both theoretically and experimentally concerns the time dependence of the the precursor width $w(t)$. The horizontal SOS model, for example, predicts [13,14] a linear time dependence for the precursor in the complete wetting regime. More general argumets give [9,11] a crossover from "adiabatic" to "diffusive" behavior, while experiments for tiny droplets have mostly been fitted to diffusive behavior [4–8]. In our case, the calculated data for $w(t)$ can be efficiently analyzed by developing a phenomenological finite size scaling law

based on the idea, that there exists a crossover towards "diffusive" behavior controlled by the pressure of the cap, and thus by the number of particles. We conjecture the following form:

$$w(t,N) = t^x \phi(t/N^y), \tag{6}$$

where the scaling function $\phi(z)$ describes the crossover. Thus, there must be a crossover time which is a function of N, viz. $t_c \sim N^y$. To obtain the correct limits for the width, the scaling function must satisfy

$$\phi(z) \sim \begin{cases} \text{const} & \text{for } z \ll 1 \\ z^{1/2-x} & \text{for } z \gg 1. \end{cases} \tag{7}$$

We can use the following arguments to limit the range of the unknown exponent y. The characteristic length scale l_c for the droplet is proportional to $\sqrt{N}$ for the ridge-shaped droplet. Minimum value of y occurs for (adiabatic) spreading with a constant velocity v, for which $t_c = l_c/v \sim \sqrt{N}$. On the other hand, if spreading were purely diffusive, $l_c = \sqrt{Dt_c}$, where D is the diffusion coefficient. Thus, we obtain $t_c \sim N$. These approximate arguments limit y between $1/2$ and 1.

In Ref. [18] the scaling law was seen to be valid for solvent particles using exponents $x = 0.9$ and $y = 0.75$. The former exponent was chosen according to the analytic law by Joanny and de Gennes [11]. The fact that $y = 0.75$ indicates that the spreading is not purely diffusive but rather caused by a combination of the pressure of the cap and collective migration of the particles. Our results for $w(t)$ show that these results hold both for solvent particles and dimers in all cases. Although for finite tetramer concentrations the droplets no longer exhibit a clearly visible crossover from almost linear to "diffusive" spreading, we find that the width of the precursor film w obeys the scaling form of Eq. (7), again with $x \approx 9/10$, and $y \approx 0.67/x \approx 0.75$. This has been verified for three cases: with tetramer concentration $c = 0.5$ for S_{III}, and $c = 1.0$ for S_{II} and S_{III}. Typical scaling functions and values of N used are depicted in Fig. 9. Within the accuracy of our data, the scaling functions are identical in all cases.

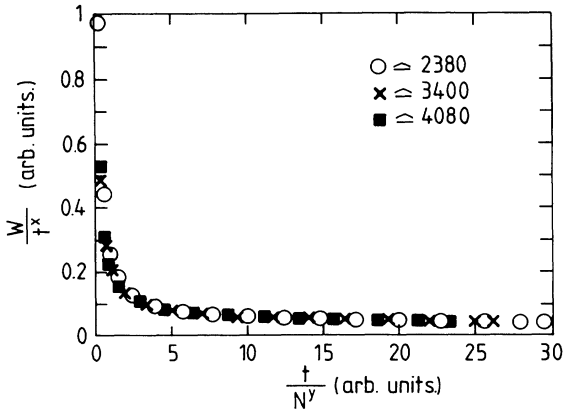

FIG. 9. Scaling functions $\phi(z)$ for pure tetramer droplets in potential S_{II}, with $N = 2380 - 4080$. Best data collapse is obtained with $x = 0.9$ and $y = 0.75$.

IV. SUMMARY AND DISCUSSION

The spreading dynamics of tiny droplets on surfaces is a fascinating phenomonon, much more complicated than originally thought. When dealing with such complicated dynamical problems at low dimensions, it should not be surprising that degrees of freedom not so relevant in the bulk can play a significant role. A good example of this is the blocked two-dimensional diffusion of short chains on surfaces, which in itself can lead to spherical droplet shapes under submonolayer conditions [5,20]. In this work, by using a simple molecular-dynamics model of mixtures of flexible chains and solvent particles, we have tried to unravel the microscopic origins for some of the different droplet morphologies seen in the experiments. In particular, we have concentrated on the possible differences in droplet morphologies caused by the chain structure of the spreading liquid, and the strength of the surface potential. These issues are particularly relevant when reasons behind dynamical layering are explored. Our results demonstrate that when the surface attraction becomes relatively weak, even relatively short polymer chains beneath the bulk entanglement regime can dynamically mix in spreading droplets, leading to more rounded droplet shapes. On the other hand, for strong attractive potentials and more isotropic particles, dynamical layering seems to be more characteristic. Although our results are valid for microdroplets only, they suggest that *both* the chain structure of the liquids *and* the details of the surface potential can play an active role under real experimental situations. It would thus be of great interest to study these and other related questions, such as the crossover scaling predicted for microdroplets, in further well-controlled systematic experiments.

ACKNOWLEDGMENTS

We wish to thank S. Herminghaus, K. Kaski, R. Swendsen, and O. Venäläinen for useful discussions. This work has been supported by the Academy of Finland.

[1] P. G. de Gennes, Rev. Mod. Phys. **57**, 827 (1985).
[2] F. Heslot, N. Fraysse, and A. M. Cazabat, Nature **338**, 640 (1989).
[3] F. Heslot, A. M. Cazabat, and P. Levinson, Phys. Rev. Lett. **62**, 1286 (1989).
[4] F. Heslot, A. M. Cazabat, P. Levinson, and N. Fraysse, Phys. Rev. Lett. **65**, 599 (1990).
[5] U. Albrecht, A. Otto, and P. Leiderer, Phys. Rev. Lett. **68**, 3192 (1992).
[6] M. P. Valignat, N. Fraysse, A. M. Cazabat, and F. Heslot,

Langmuir **9**, 601 (1993).
[7] N. Fraysse, M. P. Valignat, A. M. Cazabat, F. Heslot, and P. Levinson, J. Coll. Interface Sci. **158**, 27 (1993).
[8] J. De Coninck, N. Fraysse, M. P. Valignat, and A. M. Cazabat, Langmuir **9**, 1906 (1993).
[9] L. Leger and J. F. Joanny, Rep. Prog. Phys. **55**, 431 (1992).
[10] L. H. Tanner, J. Phys. D **12**, 1473 (1979).
[11] J. F. Joanny and P. G. de Gennes, J. Phys. **47**, 121 (1986).
[12] P. G. de Gennes and A. M. Cazabat, C. R. Acad. Sci. Paris, Ser. II **310**, 1601 (1990).
[13] D. B. Abraham, P. Collet, J. de Connick, and F. Dunlop, Phys. Rev. Lett. **65**, 195 (1990); J. Stat. Phys. **61**, 509 (1990).
[14] D. B. Abraham, J. Heiniö, and K. Kaski, J. Phys. A **24**, L309 (1991); J. Heiniö, K. Kaski, and D. B. Abraham, Phys. Rev. B **45**, 4409 (1992); E. Cheng and C. Ebner, Phys. Rev. B **45**, 12 056 (1992).
[15] O. Venäläinen, T. Ala-Nissila, and K. Kaski, Europhys. Lett. **25**, 125 (1994).
[16] J. Hautman and M. L. Klein, Phys. Rev. Lett. **67**, 1763 (1991).
[17] J.-x. Yang, J. Koplik, and J. R. Banavar, Phys. Rev. Lett. **67**, 3539 (1991).
[18] J. A. Nieminen, D. B. Abraham, M. Karttunen, and K. Kaski, Phys. Rev. Lett. **69**, 124 (1992); J. A. Nieminen, A. Lukkarinen, K. Kaski, and D. B. Abraham (unpublished).
[19] P.-G. de Gennes, *Scaling Concepts in Polymer Physics* (Cornell University Press, Ithaca, NY, 1979); M. Doi and S. F. Edwards, *The Theory of Polymer Dynamics* (Oxford University Press, Oxford, 1986).
[20] T. Hjelt and T. Ala-Nissila (unpublished).
[21] J. A. Nieminen and T. Ala-Nissila, Europhys. Lett. (to be published).
[22] W. G. Hoover, Phys. Rev. A **31**, 1695 (1985).
[23] J. P. Hansen and L. Verlet, Phys. Rev. **184**, 151 (1969).
[24] A. P. Sutton, J. B. Pethica, H. Rafii-Tabar, and J. A. Nieminen, in *Electron Theory in Alloys Design*, edited by D. G. Pettifor and A. H. Cottrell (Institute of Metals, London, 1992).
[25] A. J. C. Ladd and L. V. Woodcock, Mol. Phys. **36**, 611 (1978).